ChemComm

Triggering the Dynamics of a Carbazole-p-[phenylene-diethynyl]-xylene Rotor through a Mechanically Induced Phase Transition

Journal:	*ChemComm*
Manuscript ID	CC-COM-07-2019-005672.R2
Article Type:	Communication

COMMUNICATION

Triggering the Dynamics of a Carbazole-*p*-[phenylene-diethynyl]-xylene Rotor through a Mechanically Induced Phase Transition

Received 00th January 20xx,
Accepted 00th January 20xx

Andrés Aguilar-Granda,[a] Abraham Colin-Molina,[a] Marcus J. Jellen,[b] Alejandra Núñez-Pineda,[a,c] M. Eduardo Cifuentes-Quintal,[d] Rubén Alfredo Toscano,[a] Gabriel Merino,[d] Braulio Rodríguez-Molina*[a]

DOI: 10.1039/x0xx00000x

The new rotor 2 exhibits rich solvatomorphism behavior with eight X-ray structures obtained. A heterogeneous solid obtained by mechanical stress showed a dominant isotropic ^{2}H line shape at high temperatures. The motion occurs only in the amorphous component of this solid, with an Ea 7.4 kcal/mol and a low pre-exponential factor A = 6.22x10^{10} s^{-1}, which indicates that the motion requires the distortion of the molecular axis.

Molecular rotors are artificial molecular machines designed to show intramolecular rotation. The study of their rotational dynamics has been the focus of numerous research groups using a variety of spectroscopic techniques.[1] Crystalline molecular rotors may also show interesting properties for applications as advanced materials. The rotational component should be able to reorient under the appropriate thermal,[2] dielectric,[3] or optical influence.[4] To achieve this reorientation freely, the rotary part (*rotator*) can be surrounded by bulky groups (*stator*)[5] or it can be hosted within porous crystals.[6]
The rotational dynamics depend not only on the size and point symmetry of the rotator but also on the resulting intermolecular interactions.[7] Finding the appropriate crystal array that allows motion is a challenging task sometimes restricted by the solubility of the molecules or the stability of the crystals formed (*i.e.* unstable solvates or hydrates), and a polymorphism screening would help to uncover the desired solid form.[8]
Our group has been interested in the synthesis of crystalline fluorescent rotors using carbazole as the rigid component with potential optoelectronic applications.[9] Given its poor solubility, only one unstable solvate and one solvent-free structure of rotor **1** were obtained previously.[10] We have also shown that despite its flat architecture, carbazole allows for the rotation of the central ring in the solvent-free form with moderate rotational frequencies of 6 MHz at 295K.[10a] It is worth to mention that other components in **1** did not show motion at any explored temperature.

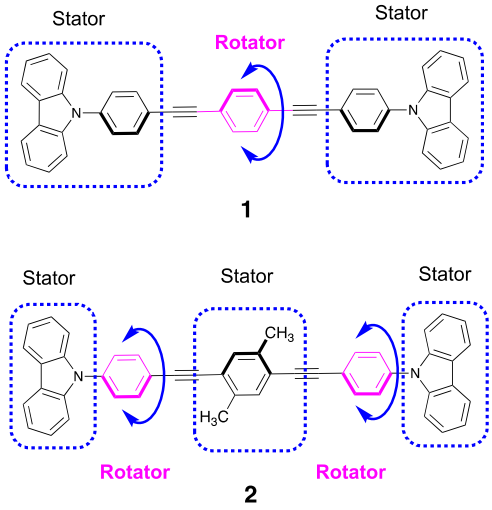

Figure 1. Chemical structures of molecular rotors **1** (previously reported) and **2** (this work). In the case of **2**, the attached methyl groups inhibit the motion of the central aromatic ring and allowed the dynamics of the rings (magenta) attached to the carbazole stator.

Based on these previous results, we wanted to perform precise but small structural changes in the rotator to deliberately stop the 2-fold flip motion of the central phenylene. To this end, we envisioned the molecular rotor **2** with a xylene derivative as the central constituent (Figure 1). The methyl groups would be large enough to hinder the rotation of the central fragment while preserving most of the electronic distribution (Figure S24).
As described below, the substitution indeed restricted the rotation of the central aromatic ring, according to variable temperature (VT) solid state ^{13}C NMR CPMAS experiments and VT X-ray studies. Gratifyingly, the methyl groups also substantially improved the solubility of **2**, which gave rise to new solid-state forms, either as multiple solvates (forms **I** to **V**) or solvent-free structures (**VI**-**VIII**).
Despite all this structural diversity and according to VT ^{2}H NMR experiments in the solid state, the rings directly attached to the carbazole fragment in **2** are *only* able to show motion in an

[a]*Instituto de Química, Universidad Nacional Autónoma de México, Circuito Exterior, Ciudad Universitaria, 04510, Ciudad de México, México.*
[b]*Department of Chemistry and Biochemistry, University of California, Los Angeles, California, 90095, United States*
[c]*Centro Conjunto de Investigación en Química Sustentable UAEM-UNAM, Carretera Toluca-Atlacomulco Km 14.5, Toluca, 50200, Estado de México, México.*
[d]*Departamento de Física Aplicada, Centro de Investigación y de Estudios Avanzados, Unidad Mérida. Km 6 Antigua Carretera a Progreso. Apdo. Postal 73, Cordemex, 97310, Mérida, Yuc., México.*
Electronic Supplementary Information (ESI) available: Experimental procedures, tables with crystallographic parameters, ^{1}H and ^{13}C NMR solution data, ^{13}C and ^{2}H solid state NMR data DSC and TGA results. (CCDC Numbers): 1940315-1940321. See DOI: 10.1039/x0xx00000x

amorphous solid that originates by applying mechanical stress to form **VII**. We describe here how this motion is allowed by the concomitant torsion of the whole structure. These findings shed light into the subtle structural differences that govern the intramolecular motion in artificial molecular machines.

Compound **2** and its deuterated derivative **2**-d_8 were synthesized by cross-coupling reactions (Scheme 1), using 4-iodophenyl-carbazole **3** or its deuterium-derivative **3**-d_8, and 1,4-diethynyl-[2,5-dimethyl-phenylene] **4**.[11] The title compounds **2** and **2**-d_8 were obtained in good yields, 64 and 68 %, respectively. The complete spectroscopic assignment of the title compounds **2** and **2**-d_8 was carried out by using 1D and 2D NMR (HSQC and HMBC, see *Supporting Information*), FTIR and mass spectrometry.

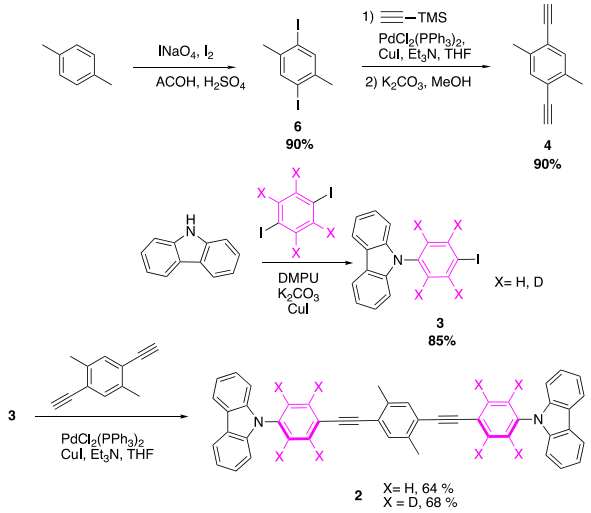

Scheme 1. Synthesis of title compound **2** and its deuterated derivative **2**-d_8.

Compared with the previously reported compound **1**, the novel compound **2** showed a much improved solubility. Slow evaporation in open vials afforded five solvates labelled **I** (toluene), **II** (chlorobenzene), **III** (*p*-xylene), **IV** (THF) and **V** ($CHCl_3$). We also obtained a solvate using dichloromethane, but due to its low thermal stability, the X-ray statistical parameters were not ideal and will be not discussed in detail.[12]

Based on the crystallographic data, we classified the solvates into two isostructural solvatomorphic groups (labelled **A** and **B** for better comparison). Group **A** contains the solvates with aromatic molecules inside the crystal lattice, as seen in Table S1. Conversely, group **B** contains the solvates of THF, chloroform (and the unstable DCM).

A comparison of representative examples of each group (forms **I** and **IV**) along with the solvent-free structure **VI** is shown in Figure 2. The supramolecular array in the group **A** propagates by means of CH···π interactions. The components of the lattice are stoichiometrically distributed (1:1), with the aromatic guest located close to one carbazole fragment, showing a CH···π interaction (Figure 2a). Conversely, in the group **B** the corresponding guests are placed in channels (Figure 2b).

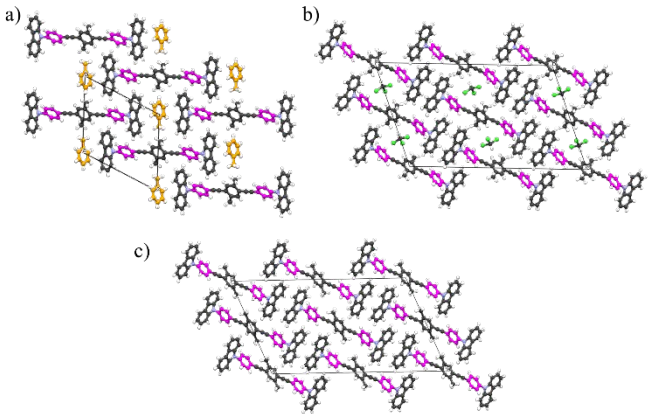

Figure 2. Packing arrays of representative examples of the solid forms reported here: a) toluene solvate **I**, b) chloroform solvate **V**. c) Solvent-free form **VI** (obtained from slow evaporation of ethyl acetate).

Being isostructural to other structures of the group **A**, the solvent-free form **VI** also showed parallel layers of molecules propagating through the CH···π interactions, but between the central *p*-xylene ring and a neighbouring carbazole fragment (Figure 2c). In this form, a significant interaction occurs between one methyl group and one adjacent carbazole component, with a C-H-π distance of 3.34 Å and angle of 166 °, which would 'lock' the potential motion of this component.

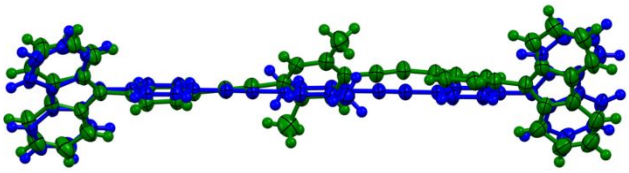

Figure 3. Superposition of the two solvent-free structures of rotor **2** that are obtained by desolvation of the solvates (form **VI**, blue) and its subsequent phase transition (form **VII**, green, only one disordered position shown). The molecular conformation becomes severely distorted upon the phase transition.

The differential scanning calorimetry (DSC) of solvent-free **VI** showed a small but clear endothermic transition close to 490 K (217 °C), and thus we investigated this further by using the hot stage microscopy (HSM). By heating fresh crystals of form **VI** above 533 K (260 °C) for 1 hour, they transform to a new form labelled **VII**. The resulting structure showed that the molecule is disordered over two positions, with a severe distortion of the molecular conformation, as it can be seen in the comparison of the two structures (Figure 3).

The solvates are stable at room temperature, showing an endothermic peak between 348 K and 423 K, which was associated to the desolvation. We confirmed this statement by performing TG analyses and powder X-ray diffraction studies of the resulting solids (see *Supplementary Information*). Based on these results, we can conclude that all solvates transform to the form **VII**.

Subsequently, the internal rotation of the xylene portion, or rather, the lack of it, was explored by variable temperature solid-state ^{13}C CPMAS NMR using the **2**-d_8 analogue so the corresponding C-D carbon atoms of the phenylene would not overlap the *p*-xylene signals on the ^{13}C CPMAS spectrum.

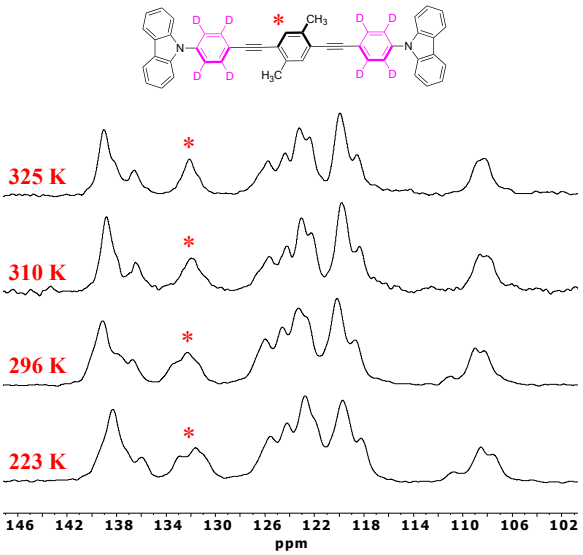

Figure 4. Variable temperature ^{13}C NMR CPMAS of rotor **2**, highlighting the changes in the carbon signals from the central xylene at low temperatures, denoted by an asterisk, see the ^{13}C peak assignment in the *Supplementary Information*.

Given the fact that the form **VII** requires some preparation of the sample (solvate and then desolvation or very high temperatures), to probe the dynamics of the xylene portion we started with form **VI.** The ^{13}C CPMAS experiments from 325 K to 223 K showed only minor changes in the chemical shifts of the xylene component, which were attributed to small oscillations of this ring (Figure 4). We corroborated this by collecting X-ray structures at different temperatures, where no major changes were observed (Figure S4)

We also carried out VT ^{2}H NMR studies by the spin echo technique to document the behaviour of the ring adjacent to the carbazole. Deuterium is a sensitive quadrupolar nucleus, so changes in the crystallographic environment caused by the reorientation of C-D bond with respect to the external magnetic field will produce changes in the broad line shape, known as the Pake pattern.[13] Here we emphasize that this ring did not show motion at any explored temperature in the previously reported rotor **1**, so we did not expect rotation in this component.

We started with selected structures of the two groups, the solvates **I** (toluene, group A) and **V** (chloroform, group B). The experiments from room temperature up to 380 K (before desolvation), showed a broad ^{2}H line shape that is characteristic of a static segment.[14]

The solvent within the crystals was removed by heating the solvates at 423 K in a hot plate for 30 min, causing them to transform to the form **VII**. After this procedure, the deuterated phenylenes were still static. Considering that traces of the solvent could be obstructing the motion, we ground the solid using an agate mortar for 10 minutes. The resulting solid was evaluated by powder X-ray diffraction and compared with the known solvent-free forms **VI** and **VII**.

Unexpectedly, the mechanical treatment generated a heterogeneous solid with crystalline and amorphous components. The crystalline part was different from the previous solids and it was labelled **VIII**. To date, we have not been able to obtain single crystals of this form, but DFT computations helped us postulate a structure that reproduces very well the observed X-ray diffraction pattern (see *Supplementary Information* for details).

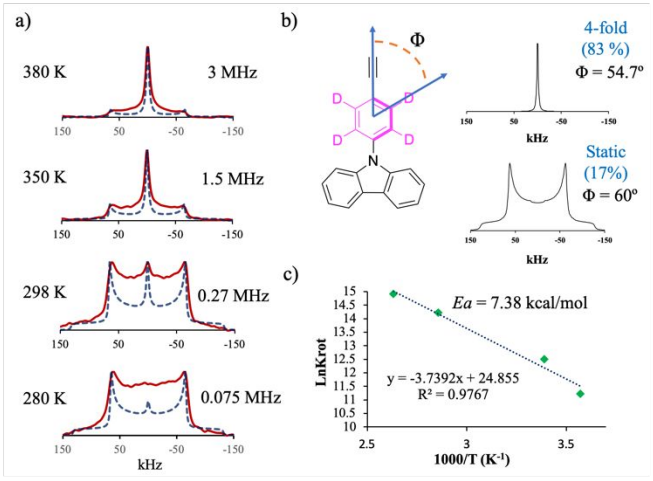

Figure 5. a) Experimental (solid line) and simulated (dotted-line) VT ^{2}H NMR spectra of **2**-d_8, a solid with 83% amorphous (rotation in kHz) and 17 % (static) components. b) Cone angles used to describe the rotation of the phenylene c) Arrhenius plot of Ln K_{rot} vs 1/T.

The new solid showed a promising narrow peak that suggested motion. Heating up to 380 K made the isotropic line shape dominant (Figure 5a). It is worth to note that depending on the time and strength of the milling of **2**, we produced mixtures with decreasing amounts of the crystalline component (batches A, B and C)[15] and in each case the narrow signal was less visible.

The isotropic ^{2}H line shape in rotating 1,4-disubstituted phenylenes requires the distortion of the molecular axis from 60º to 54.7º and the existence of multiple minima (> 3-fold) as reported previously.[16] DFT computations in the gas and in the solid-state corroborated the presence of a four-fold rotational potential and the twist of the molecular axis (Figure S25 and Movies S1-S3).

Considering the above, the deuterium experimental line shapes in this work were successfully reproduced by using a model based on 4-fold jumps over a symmetric rotational potential (Figure 5b). It is important to note that the amount of the crystalline component in each batch was taken into account as the static component for the line shape.

The batch with the largest amorphous content (83%), showed an activation energy of rotation of E_a= 7.38 kcal/mol and a pre-exponential factor of A = 6.22 x 10^{10} s^{-1} (Figure 5c). As the amount of the crystalline component in the heterogenous solid increases, the isotropic line shape is less evident and is overlapped by the static Pake pattern. The fittings of the other batches afforded slightly higher E_a and A values (see Figures S20-S23 and Table S3). The trend indicates that the rotation occurs only in the amorphous component.

Interestingly, the low pre-exponential factor in the batch A reveals a geometrically congested transition state, implying that the motion in **2** depends on the collective bending of the molecule during the phenylene angular displacements. A DFT calculation (Figure S25) indicates that the rotor requires 6 kcal/mol to rotate in the gas phase, so the amorphous nature of

the ground solid enables the motion by providing a very fluid environment.

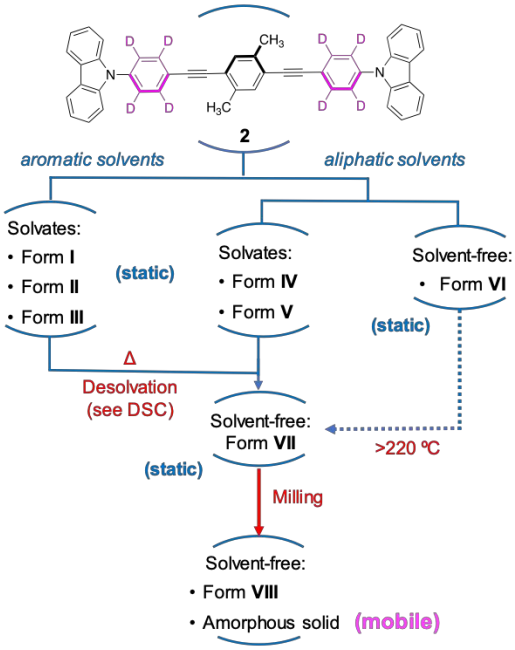

Chart 1. A condensed view of the observed solid forms of **2** their solid-to-solid transformations and the associated internal behaviours.

In summary, exchanging a central phenylene for a xylene ring increases the solubility of the compound and gives rise to several solid forms that were characterized by X-ray diffraction (Chart 1). The methyl groups also inhibited the rotation of the central ring, as corroborated by VT ^{13}C NMR CPMAS. Interestingly, the phenylene rings attached to the carbazole showed motion after grinding the crystals, a process that produces an heterogenous solid (amorphous/crystalline) with an isotropic ^{2}H NMR signal in the solid state. The motion in the solid occurs only in the amorphous component, and in a sample with 17 % crystalline component, a low activation barrier to rotation (E_a = 7.38 kcal/mol) was observed, requiring a bent structure with a low pre-exponential factor (A = 6.22 x 10^{10} s^{-1}).

Conflicts of interest

There are no conflicts to declare

We thank the financial support from PAPIIT IN209119 and CONACYT for the PhD scholarship (A.C.-M.). We acknowledge the UCLA Department of Chemistry and Biochemistry for solid state ^{2}H NMR experiments (NSF DMR-1700471 and MRI-1532232). We thank the technical assistance from Dr. Diego Martínez-Otero (X-ray), Dra. María del Carmen García Gonzalez, María de los Ángeles Peña González, and M. Sc. Elizabeth Huerta Salazar (MS and NMR). We thank Prof. Salvador Pérez-Estrada for initial solid-state NMR measurements.

Notes and references

1 (a) M. E. Howe, M. A. Garcia-Garibay, J. Org. Chem. DOI: 10.1021/acs.joc.9b00993; (b) L. Catalano, P. Naumov, CrystEngComm, 2018, **20**, 5872-5883; (c) M. Inukai, T. Fukushima, Y. Hijikata, N. Ogiwara, S. Horike, S. Kitagawa, J, Am. Chem. Soc., 2015, **137**, 12183-12186. (d) G. S. Kottas, L. I. Clarke, D. Horinek, J. Michl, Chem. Rev., 2005, **105**, 1281−1376. (e) A. Comotti, S. Bracco, A. Yamamoto, M. Beretta, T. Hirukawa, N. Tohnai, M. Miyata, P. Sozzani, J. Am. Chem. Soc., 2014, **136**, 618-621. (f) W. Setaka, K. Yamaguchi, J. Am. Chem. Soc., 2012, **134**, 12458.

2 S. Kharel, H. Joshi, N. Bhuvanesh, J. A. Gladysz, Organometallics, 2018, **37**, 2991−3000.

3 (a) Z.-X. Zhang, T. Zhang, W.-Y. Zhang, P.-P. Shi, Q. Ye, D.-W. Fu, Inorg. Chem., 2019, **58**, 4600−4608; (b) M. Tsurunaga, Y. Inagaki, H. Momma, E. Kwon, K. Yamaguchi, K. Yoza, W. Setaka, Org. Lett., 2018, **20**, 6934−6937. (c) S. Bracco, M. Beretta, A. Cattaneo, A. Comotti, A. Falqui, K. Zhao, C. Rogers, P. Sozzani, Angew. Chem. Int. Ed., 2015, **54**, 4773-4777. (d) L. Kobr, K. Zhao, Y. Shen, A. Comotti, S. Bracco, R. K. Shoemaker, P. Sozzani, N. A. Clark, J. C. Price, C. T. Rogers, J. Michl, J. Am. Chem. Soc., 2012, **134**, 10122-10131.

4 (a) J. Dong, X. L., S. B. Peh, Y. D. Yuan, Y. Wang, D. Ji, S. Peng, G. Liu, S. Ying, D. Yuan, J. Jiang, S. Ramakrishna, D. Zhao, Chem. Mater., 2019, **31**, 146−160, (b) J. Dong, A. K. Tummanapelli, X. Li, S. Ying, H. Hirao, D. Zhao, Chem. Mater., 2016, **28**, 7889-7897. (c) M. Cipolloni, J. Kaleta,M. Mašát, P. I. Dron, Y. Shen, K. Zhao, C. T. Rogers, R. K. Shoemaker, J. Michl, J. Phys. Chem. C, 2015, **119**, 8805-8820.

5 Z. J. O'Brien, S. D. Karlen, S. Khan, M. A. Garcia-Garibay, J. Org. Chem., 2010, **75**, 2482–2491

6 A. Comotti, S. Bracco, P. Sozzani, Acc. Chem. Res., 2016, **49**, 1701−1710.

7 M. K. Dudek, S. Kazmierski, M. Kostrzewa, M. J.Potrzebowski, *Chapter One - Solid-State NMR Studies of Molecular Crystals,* Annual Reports on NMR Spectroscopy, 2018, **15**, 1-81.

8 Y. A. Abramov, M. Zell, J. F. Krzyzaniak, *Toward a rational solvent selection for conformational polymorph screening*. Chemical engineering in the pharmaceutical industry: Active pharmaceutical Ingredients, Second edition, John Wiley & Sons, Inc., 2019.

9 W. Bernal, O. Barbosa-García, A. Aguilar-Granda, E. Pérez-Gutiérrez, J.-L. Maldonado M. J. Percino, B. Rodríguez-Molina, Dyes Pigm., 2019, **163**, 754-760.

10 (a) A. Aguilar-Granda, S. Perez-Estrada, A. E. Roa, J. Rodríguez-Hernández, S. Hernández-Ortega, M. Rodriguez, B. Rodríguez-Molina, Cryst. Growth Des., 2016, **16**, 3435−3442; (b) A. Aguilar-Granda, S. Perez-Estrada, E. Sanchez-González, J. R. Álvarez, J. Rodríguez-Hernández, M. Rodríguez, A. E. Roa, S. Hernández-Ortega, I. A. Ibarra, B. Rodríguez-Molina, J. Am. Chem. Soc., 2017, **139**, 7549−7557.

11 M. M. Haley, Modern Alkene Chemistry. Catalytic and Atom-Economic Transformations, Angew. Chem., Int. Ed., 2015, **54**, 8332.

12 Preliminary unit cell parameters: a)32.44 (4) Å, b) 5.75 (3) Å, c) 21.65 (3) Å, α) 90°, β) 110.74° (3), γ) 90°.

13 M. J. Duer, *Introduction to Solid-State NMR Spectroscopy*, Blackwell, Oxford, United Kingdom, 2004.

14 T. R. Molugu, S. Lee, M. F. Brown, Chem. Rev., 2017, **117**, 12087−12132.

15. Three different batches of rotor **2** were ground and a mixture of crystalline/amorphous components was always present: batch A (17%/83%), batch B (24%/76%) and batch C (42%/58%), see also Supplementary Information for their corresponding VT ^{2}H spectra.

16. A. Colin-Molina, M. J. Jellen, E. García-Quezada, M. E. Cifuentes-Quintal, F. Murillo, J. Barroso, S. Perez-Estrada, R. A. Toscano, G. Merino, B. Rodríguez-Molina, Chem. Sci., 2019, **10**, 4422–4429;

Table of Contents Entry

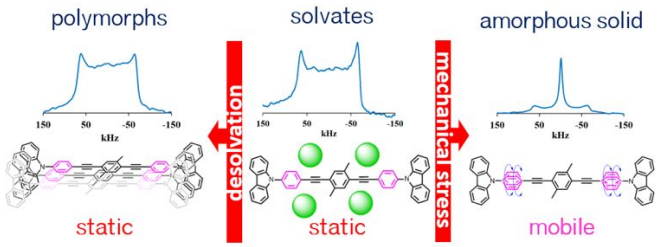

A crystalline molecular machine with several solid phases where only one is able to show intramolecular rotation